Higher-genus *su*(*N*) fusion multiplicities as polytope volumes

2002 J. Phys. A: Math. Gen. 35 10129

(http://iopscience.iop.org/0305-4470/35/47/312)

INSTITUTE OF PHYSICS PUBLISHING JOURNAL OF PHYSICS A: MATHEMATICAL AND GENERAL

J. Phys. A: Math. Gen. **35** (2002) 10129–10147 PII: S0305-4470(02)53252-2

Higher-genus $su(N)$ fusion multiplicities as polytope volumes

G Flynn[1], **J Rasmussen**[2], **M Tahić**[1] **and M A Walton**[1]

[1] Physics Department, University of Lethbridge, Lethbridge, Alberta, Canada T1K 3M4
[2] CRM, Université de Montréal, Case postale 6128, succursale centre-ville, Montréal, Québec, Canada H3C 3J7

E-mail: flynngt@uleth.ca, rasmusse@crm.umontreal.ca, tahimk@uleth.ca and walton@uleth.ca

Received 9 September 2002
Published 12 November 2002
Online at stacks.iop.org/JPhysA/35/10129

Abstract

We show how higher-genus $su(N)$ fusion multiplicities may be computed as the discretized volumes of certain polytopes. The method is illustrated by explicit analyses of some $su(3)$ and $su(4)$ fusions, but applies to all higher-point and higher-genus $su(N)$ fusions. It is based on an extension of the realm of Berenstein–Zelevinsky triangles by including so-called gluing and loop-gluing diagrams. The identification of the loop-gluing diagrams is our main new result, since they enable us to characterize higher-genus fusions in terms of polytopes. Also, the genus-2 0-point $su(3)$ fusion multiplicity is found to be a simple binomial coefficient in the affine level.

PACS numbers: 02.20.−a, 02.10.Hh

1. Introduction

Recently, methods have been developed for computing $su(N)$ tensor product [1, 2] and fusion [3, 4] multiplicities based on a generalization of the Berenstein–Zelevinsky (BZ) triangles [5]. The idea is to associate a convex polytope to a multiplet of integrable highest weights $(\lambda, \ldots, \sigma)$. The discretized volume of the polytope is the (tensor product or) fusion multiplicity associated with the coupling of the weights $(\lambda, \ldots, \sigma)$ to the singlet.

Rasmussen and Walton [1] describe ordinary three-point tensor products, while [2] extends the results to higher-point couplings. The extension is obtained by introducing a *gluing* of BZ triangles, whereby the triangular configurations are replaced by multi-sided configurations or diagrams.

The dependence on the affine level in fusion may be implemented by associating threshold levels to the tensor product couplings [6]. Using that idea in the framework of BZ triangles, allows one to also characterize fusion multiplicities by polytopes. The extra input is an assignment of threshold levels to the BZ triangles. That is trivial for $su(2)$, straightforward

for $su(3)$ [7], somewhat complicated for $su(4)$ [8], but believed to be possible for all $su(N)$. Polytope characterizations of fusion multiplicities have been studied in [3, 4, 9]: $\mathcal{N}$-point $su(2)$ and $osp(1|2)$ fusions are treated in [2] and [9], respectively, while [4] discusses three-point $su(3)$ and $su(4)$ fusions. One objective of the present work is the extension of the latter results to higher-point fusions.

Higher-genus fusions may also be characterized by polytopes. The appearance of loops forces us to introduce a new class of diagrams. We shall call them *loop-gluing diagrams*, or for short, *loop gluings*. In the case of $su(2)$, they were introduced in [3], leading to a characterization of all higher-genus $\mathcal{N}$-point $su(2)$ fusions by convex polytopes. This was extended to $osp(1|2)$ in [9], and the second objective of the present work is the extension of it to $su(N)$. The main results are the identification of the $su(N)$ loop gluings (illustrated for $su(4)$ in (11)), and the explicit characterization of higher-genus $\mathcal{N}$-point $su(3)$ and $su(4)$ fusion multiplicities as discretized volumes of certain polytopes.

The characterization of fusion multiplicities as the discretized volume of polytopes, makes manifest that the multiplicities are non-negative integers. That is *a priori* not clear when examining the Verlinde formula [10]. Furthermore, the geometrical interpretation offers a better understanding of the underlying symmetries and properties of the multiplicities and their level-dependence. As an example, in [4] it was conjectured that for a fixed triplet of $su(N)$ weights (λ, μ, ν), the threshold multiplicity has at most one local maximum as a discrete function of the threshold level. We recall that the threshold multiplicity [11] is the number of different couplings of the weights (λ, μ, ν) with the same threshold level.

As a computational advantage of our description we mention that it results in fast computer programs, when the discretized volumes of the polytopes are measured in terms of multiple-sum formulas. The latter also provide very explicit formulas for the multiplicities, as opposed to the well-known combinatorial ones, such as the Littlewood–Richardson rule for tensor products, for example. More conjecturally, the geometrical interpretation may help towards an extended Littlewood–Richardson rule for fusion.

Our results are of a high technical complexity. For the benefit of this presentation, we thus focus on examples and only allude to the general case. It is straightforward to describe, though. After a brief discussion of BZ triangles and the method of gluing, we introduce the loop-gluing diagrams in section 2. An application is considered in section 3 where we examine the genus-1 $\mathcal{N}$-point $su(3)$ fusion multiplicities for generic non-negative integer level. The genus-2 0-point $su(3)$ fusion multiplicity is worked out explicitly and found to be a simple binomial coefficient in the affine level. This is believed to be the first concise result on fusion multiplicities for rank and genus both higher than one. In section 4 we describe the extension to higher-genus and higher-rank $su(N)$. We pay particular attention to genus-1 0-point fusions for higher rank. Section 5 contains some concluding remarks, while the appendix provides details on higher-genus $su(4)$ fusion multiplicities, with particular emphasis on the genus-1 1-point and genus-2 0-point fusions.

2. Triangles, gluings and loops

Let us briefly review some results of [1–4]. We refer to these papers for details.

A BZ triangle is a triangular arrangement of non-negative integers subject to certain constraints: the outer constraints depending on the three $su(N)$ weights (λ, μ, ν), and the hexagon identities which are consistency conditions. According to [5], the number of possible BZ triangles determines the associated tensor product multiplicity $T_{\lambda,\mu,\nu}$.

By relaxing the constraint that all the $E_r = \frac{3}{2}r(r+1)$ integer entries are non-negative, one may express any such generalized BZ triangle $\mathcal{T}$ as the linear combination [1]

$$\mathcal{T} = \mathcal{T}_0 + \sum_{i,j\geqslant 1}^{i+j=r} v_{i,j}\mathcal{V}_{i,j}. \tag{1}$$

Here r is the rank of $su(r+1)$, while $\{\mathcal{V}_{i,j}\}$ is the set of associated virtual triangles—one for each of the $H_r = r(r-1)/2$ hexagons. $\mathcal{T}_0$ is an initial (generalized BZ) triangle, and the linear coefficients $v_{i,j}$ are integers. A convenient choice of initial triangle may be found in [1]. A simple choice of labelling of the virtual triangles follows from

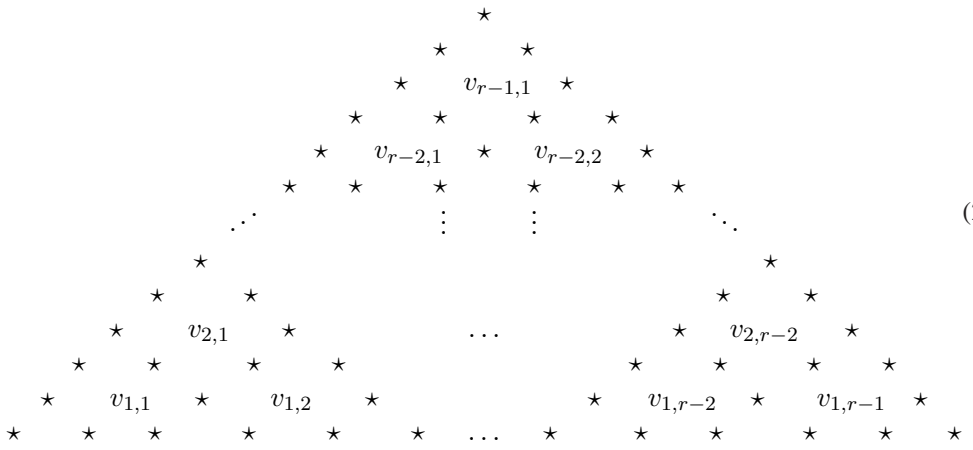

(2)

A $\star$ denotes an unspecified entry, and we see the hexagon structures surrounding each of the linear coefficients. The virtual triangles correspond to the simple distribution

$$\begin{array}{ccccccc} & & & 1 & & & \\ & & \bar{1} & & \bar{1} & & \\ 1 & \bar{1} & & & & \bar{1} & 1 \\ & & \bar{1} & & \bar{1} & & \\ 1 & \bar{1} & & & & \bar{1} & 1 \\ & & & 1 & & & \end{array} \tag{3}$$

of plus and minus ones ($\bar{1} \equiv -1$) to any given hexagon. All other entries are zero. Re-imposing the constraint that all entries of $\mathcal{T}$ (1) must be non-negative, results in a set of inequalities in $\{v_{i,j}\}$. They define a convex polytope, whose discretized volume is $T_{\lambda,\mu,\nu}$ [1]. A BZ triangle with all entries of *non-negative* integers is called a true BZ triangle.

Higher-point tensor products may be treated by gluing triangles together. The idea stems from the well-known decomposition

$$T_{\lambda,\mu,\nu,\sigma} = \sum_{\tau} T_{\lambda,\mu,\tau}T_{\nu,\sigma,\tau^+} \tag{4}$$

where τ^+ is the weight conjugate to τ. In terms of diagrams we have

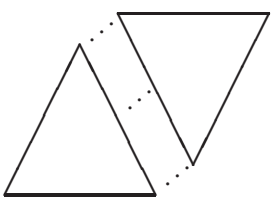

(5)

where each of the triangles represent a BZ triangle. Along the glued interface, indicated by dotted lines, the weights must match. We recall that the three weights (λ, μ, ν) of a coupling to the singlet are related as $\lambda + \mu - \nu^+ = \sum_{i=1}^{r} n_i \alpha_i$ with $n_i \in \mathbb{Z}_{\geqslant}$. $\{\alpha_i \mid i = 1, \ldots, r\}$ is the set of simple roots. Thus, we are led to introduce *gluing diagrams* or *gluing roots*, which correspond to combining the two BZ triangles (as in (5)) associated with the couplings $(0, 0, \alpha_i)$ and $\left(0, 0, \alpha_i^+\right)$, respectively. Let us illustrate the general construction [2] by listing the two gluing roots for $su(3)$:

$$\mathcal{G}_1 = \begin{array}{ccccccccc} & & & & 0 & & 0 & & 0 & & 0 \\ & & & \iddots & & & & & & & \\ & & 0 & & & \bar{1} & & & & 0 & \\ & & & \iddots & & & & & & & \\ & 0 & & & \bar{1} & & & 1 & & \bar{1} & \\ & & & & & \iddots & & & & & \\ 0 & & & & 1 & & & & 1 & & \\ & & & & & & \iddots & & & & \\ 0 & & 0 & & \bar{1} & & 1 & & & & \end{array} \tag{6}$$

$$\mathcal{G}_2 = \begin{array}{ccccccccc} & & & & 1 & & \bar{1} & & 0 & & 0 \\ & & & \iddots & & & & & & & \\ & & 1 & & & 1 & & & & 0 & \\ & & & \iddots & & & & & & & \\ & \bar{1} & & & 1 & & & \bar{1} & & 0 & \\ & & & & & \iddots & & & & & \\ 0 & & & & \bar{1} & & & & 0 & & \\ & & & & & & \iddots & & & & \\ 0 & & 0 & & 0 & & 0 & & & & \end{array} .$$

The extension to $\mathcal{N}$-point couplings, $\mathcal{N} > 4$, is straightforward. We are thus extending triangles to $\mathcal{N}$-sided diagrams $\mathcal{D}$, and (1) is replaced by

$$\mathcal{D} = \mathcal{D}_0 + \sum_{a=1}^{\mathcal{N}-2} \sum_{i,j \geqslant 1}^{i+j=r} v_{i,j}^{(a)} \mathcal{V}_{i,j}^{(a)} - \sum_{a=1}^{\mathcal{N}-3} \sum_{i=1}^{r} g_i^{(a)} \mathcal{G}_i^{(a)}. \tag{7}$$

The initial diagram $\mathcal{D}_0$ is easily described, see [2]. The label a runs over the participating triangles or gluings, respectively, while the sign in front of the last term merely is for convenience.

Fusion multiplicities are determined from the tensor product multiplicities and the associated multi-set of threshold levels $\{t\}$ [6]. In order to extend our polytope characterization of tensor product multiplicities to fusion multiplicities, we need a prescription for assigning a threshold level to a BZ triangle. That is trivial for $su(2)$, and was worked out for $su(3)$ in [7] and for $su(4)$ in [8]. The extension to higher rank is not known explicitly, but believed to exist.

Assigning a threshold level t to a triangle $\mathcal{T}$ amounts to expressing t in terms of the entries of $\mathcal{T}$. In the known cases, t is given as a maximum over simple expressions in the entries. This leads straightforwardly to a refinement of the polytope associated with the underlying tensor product coupling, by introducing inequalities depending on (and hence incorporating) the dependence on the affine level k. The procedure will be illustrated explicitly below.

To treat higher-genus fusion, we need to understand how loops appear at the level of our diagrams. It is sufficient to focus on the 'self-gluing' or tadpole:

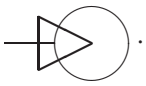

(8)

The dual picture of ordinary (Feynman-like) graphs is shown in thinner lines. Let us consider $su(2)$ first, in which case the associated *loop-gluing diagram* is

(9)

It is stressed that it differs radically from the $su(2)$ gluing root

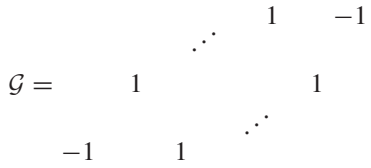

(10)

since it adds only *one* to the internal weight and not two. This discrepancy follows from the fact that the Dynkin labels satisfy $\lambda_1 + \mu_1 + \nu_1 \in 2\mathbb{Z}_{\geqslant}$, so if two weights are changed simultaneously and equally, we can only require an even change of the *sum* of the Dynkin labels.

In general, the number of independent loop-gluing diagrams is r—one for each of the Dynkin labels that must be identified along the self-gluing. To keep the presentation simple, we list here the three diagrams associated with $su(4)$:

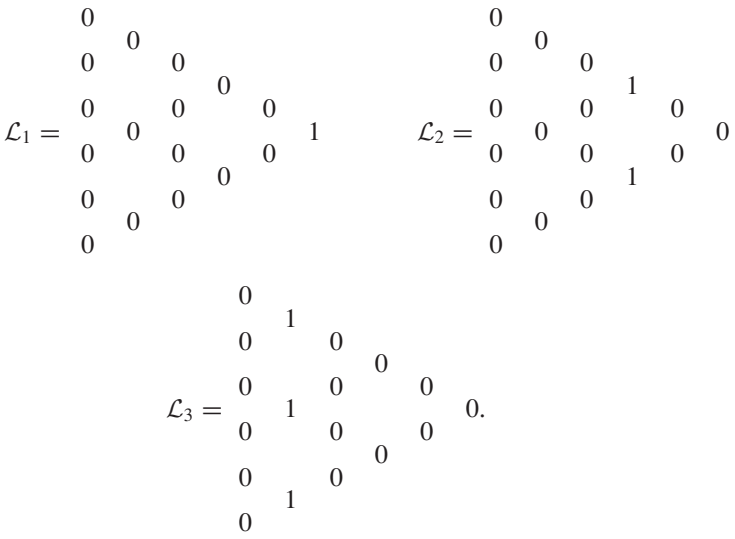

(11)

The extension to higher rank is obvious. It amounts to introducing a diagram with ones in a vertical line (when the triangle is tilted as in (11)), while all other entries are zero. The r relevant vertical lines are the first, the third, the fifth, etc, when counting from the rightmost vertex.

We are now in a position to discuss general genus-h $\mathcal{N}$-point fusions. The only missing information is how to assign explicitly a threshold level to a generic $su(N)$ BZ triangle. As already mentioned, that is known for $N \leqslant 4$, so in the following we will focus on $su(3)$ and $su(4)$. We will also allude to the straightforward but technically elaborate extension to higher rank. For results on $su(2)$, we refer to [3].

3. Higher-genus $su(3)$ fusion

A generic $su(3)$ BZ triangle may be written as

$$\begin{array}{ccccc} & & m_{13} & & \\ & n_{12} & & l_{23} & \\ m_{23} & & & & m_{12} \\ n_{13} & l_{12} & & n_{23} & l_{13} \end{array} \tag{12}$$

with outer constraints

$$\begin{aligned} &m_{13}+n_{12}=\lambda_1 \qquad n_{13}+l_{12}=\mu_1 \qquad l_{13}+m_{12}=\nu_1 \\ &m_{23}+n_{13}=\lambda_2 \qquad n_{23}+l_{13}=\mu_2 \qquad l_{23}+m_{13}=\nu_2. \end{aligned} \tag{13}$$

The hexagon identities are

$$\begin{aligned} &n_{12}+m_{23}=n_{23}+m_{12} \\ &m_{12}+l_{23}=m_{23}+l_{12} \\ &l_{12}+n_{23}=l_{23}+n_{12} \end{aligned} \tag{14}$$

of which only two are independent. The threshold level assigned to (12) is [7]

$$t=\max\{\lambda_1+\lambda_2+l_{13},\,\mu_1+\mu_2+m_{13},\,\nu_1+\nu_2+n_{13}\}. \tag{15}$$

Denoting the level of the affine $su(3)$ by k, the affine condition

$$t \leqslant k \tag{16}$$

supplements the inequalities defining the tensor product polytope. Thus, the discretized volume of the convex polytope defined by the inequalities in v

$$\begin{aligned} 0 \leqslant\ & \lambda^1-\lambda^2-\mu^1+\nu^2+v,\ \lambda^1+\mu^1-\nu^2-v,\ \lambda_2-v,\ v,\ \mu_1-v, \\ & \lambda^2+\mu^2-\nu^1-v,\ -\lambda^2-\mu^1+\mu^2+\nu^1+v,\ \lambda^2+\mu^1-\mu^2-\nu^1+\nu^2-v, \\ & -\lambda^1+\lambda^2+\mu^1-\nu^1+\nu^2-v,\ k-\lambda^1+\mu^1-\mu^2-\nu^1-v, \\ & k-\lambda^1+\lambda^2-\mu^2-\nu^2-v,\ k-\nu_1-\nu_2-v \end{aligned} \tag{17}$$

is the fusion multiplicity $N^{(k)}_{\lambda,\mu,\nu}$. The choice of initial diagram $\mathcal{D}_0$ is implicitly given in (17), and the volume is easily measured explicitly [4]. The dual Dynkin labels λ^i, μ^i and ν^i can be written in terms of ordinary Dynkin labels as $\lambda^1=\frac{1}{3}(2\lambda_1+\lambda_2)$ and $\lambda^2=\frac{1}{3}(\lambda_1+2\lambda_2)$, and similarly for μ^i and ν^i. The weights are subject to the condition

$$\lambda^i+\mu^i+\nu^i \in \mathbb{Z}_{\geqslant} \qquad i=1,2. \tag{18}$$

Let us now consider genus-1 $\mathcal{N}$-point $su(3)$ fusion multiplicities $N^{(k,1)}_{\lambda^{(1)},\ldots,\lambda^{(\mathcal{N})}}$. There is a threshold level associated with each participating triangle. Thus, there is a level-dependent inequality like (16) associated with each triangle. For $h=\mathcal{N}=1$, the tadpole (8) with outer weight λ may be expressed as

$$\mathcal{D}=\mathcal{D}_0+v\mathcal{V}-\sum_{i=1}^{2} l_i\mathcal{L}_i. \tag{19}$$

The associated convex polytope (in v, l_1 and l_2) is defined by

$$\begin{aligned}0 \leqslant\ & \tfrac{1}{3}(2\lambda_1+\lambda_2)+v,\ \tfrac{1}{3}(\lambda_1-\lambda_2)-v,\ -\tfrac{1}{3}(\lambda_1-\lambda_2)-v,\ \tfrac{1}{3}(\lambda_1+2\lambda_2)+v,\ \tfrac{1}{3}(\lambda_1-\lambda_2)\\ & -v+l_2,\ -v,\ v+l_1,\ -v+l_2,\ k-\lambda_1-\lambda_2-l_1-l_2-v,\\ & k-\lambda_1-\lambda_2-v-l_1,\ k-\tfrac{1}{3}(4\lambda_1+2\lambda_2)-l_1-l_2-v. \end{aligned} \tag{20}$$

The explicit choice of initial diagram $\mathcal{D}_0$ is easily read off (20). It follows that the multiplicity $N_\lambda^{(k,1)}$ can be written in simplified form as

$$N_\lambda^{(k,1)} = \tfrac{1}{2}(\min\{\lambda_1,\lambda_2\}+1)(k+2-\max\{\lambda_1,\lambda_2\})(k+1-\lambda_1-\lambda_2) \tag{21}$$

with $\lambda^1 \in \mathbb{Z}_{\geqslant}$ and $\lambda_1+\lambda_2 \leqslant k$. The multiplicity $N_\lambda^{(k,1)}$ vanishes if these conditions are not satisfied. Note that $\lambda^1 \in \mathbb{Z}_{\geqslant}$ implies $\lambda^2 \in \mathbb{Z}_{\geqslant}$.

We can use (21) to calculate the multiplicity of the genus-1 $\mathcal{N}$-point fusion. It is convenient to distinguish between even $\mathcal{N}$ and odd $\mathcal{N}$. The reason for this is that the triangle corresponding to the last point or outer weight $\lambda^{(\mathcal{N})}$ can have two different orientations before it is glued to the tadpole. The following diagram shows the genus-1 $\mathcal{N}$-point fusion (in this example $\mathcal{N}$ is assumed even):

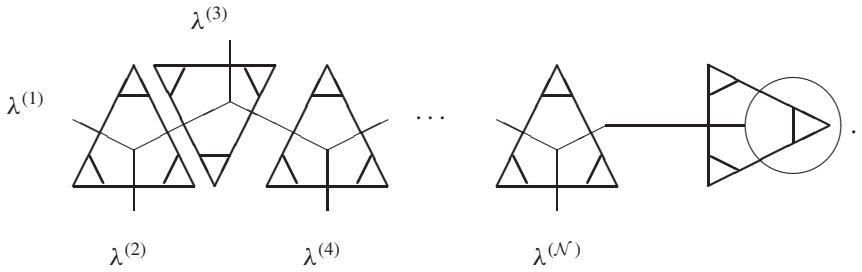

(22)

Let us introduce the parameter $\mathcal{B}$ counting—from the left of the diagram—the number of pairs of triangles not involving $\lambda^{(1)}, \lambda^{(2)}, \lambda^{(3)}$ or $\lambda^{(\mathcal{N})}$: $\mathcal{N} = 4+2\mathcal{B}$, i.e. $\mathcal{B} = \frac{1}{2}(\mathcal{N}-4)$. We also introduce the abbreviation

$$\lambda^{(1,m)} = \lambda^{(1)} + \lambda^{(2)} + \cdots + \lambda^{(m)} \tag{23}$$

The diagram associated with (22) may be written as

$$\mathcal{D} = \mathcal{D}_0 + \sum_{i=0}^{\mathcal{B}+1} v_i\mathcal{V}_i + \sum_{j=1}^{\mathcal{B}+1} u_j\mathcal{U}_j - \sum_{k=1}^{\mathcal{B}+2} s_k\mathcal{S}_k - \sum_{l=1}^{\mathcal{B}+2} r_l\mathcal{R}_l - \sum_{m=1}^{\mathcal{B}+1} g_m\mathcal{G}_m - \sum_{n=1}^{\mathcal{B}+1} f_n\mathcal{F}_n. \tag{24}$$

A $\mathcal{V}$ represents a virtual triangle associated with an upward-pointing triangle, with $\mathcal{V}_0$ being associated with the leftmost triangle. Also labelling from the left, a $\mathcal{U}$ represents a virtual triangle associated with a downward-pointing triangle. $\mathcal{R}$ and $\mathcal{S}$ are the gluing diagrams to the right of an upward-pointing triangle, $\mathcal{R}$ being the upper one, while $\mathcal{F}$ and $\mathcal{G}$ are the gluing diagrams to the right of a downward-pointing triangle, $\mathcal{F}$ being the upper one. The labelling is again from left to right. This results in the following polytope-defining list of inequalities:

$$\begin{aligned}0 \leqslant\ & \lambda_1^{(2)}+v_0-s_1,\ s_1-v_0,\ \lambda_2^{(2)}-v_0,\ k-\lambda_1^{(2)}-\lambda_2^{(2)}-\lambda_2^{(1)}+r_1-v_0\\ 0 \leqslant\ & v_0,\ \lambda_1^{(1)}-v_0,\ r_1-v_0,\ k-\lambda_1^{(1)}-\lambda_2^{(1)}-\lambda_1^{(2)}+s_1-v_0\\ 0 \leqslant\ & \lambda_2^{(1)}+v_0-r_1,\ \lambda_2^{(2)}-v_0-r_1+s_1,\ \lambda_1^{(1)}-v_0+r_1-s_1,\\ & k-\lambda_2^{(1)}-\lambda_2^{(2)}-\lambda_1^{(2)}-\lambda_1^{(1)}+r_1+s_1-v_0\end{aligned}$$

$$\vdots$$

$$
\begin{aligned}
0 &\leqslant \lambda_1^{(2b+2)} + v_b - s_{b+1}, s_{b+1} - v_b, \lambda_2^{(2b+2)} - v_b + g_b,\\
&\qquad k - \lambda_2^{(1,2b+2)} - \lambda_1^{(1,2b+2)} + r_{b+1} + s_{b+1} - v_b + g_b\\
0 &\leqslant v_b - g_b, \lambda_1^{(1,2b+1)} - v_b - g_b + f_b, g_b - v_b - f_b + r_{b+1},\\
&\qquad k - \lambda_1^{(2b+2)} - \lambda_2^{(1,2b+2)} - v_b + f_b + r_{b+1}\\
0 &\leqslant \lambda_2^{(1,2b+1)} + v_b - f_b - r_{b+1}, \lambda_2^{(2b+2)} - v_b + f_b - r_{b+1} + s_{b+1}, \lambda_1^{(1,2b+1)} - v_b + r_{b+1} - s_{b+1},\\
&\qquad k - \lambda_1^{(1,2b+2)} - \lambda_2^{(1,2b+1)} + g_b + f_b - v_b + s_{b+1}\\
0 &\leqslant \lambda_2^{(2b+1)} + u_b - f_b, \lambda_2^{(1,2b)} - u_b - f_b + g_b, \lambda_1^{(2b+1)} - u_b + f_b - g_b + s_b,\\
&\qquad k - \lambda_1^{(1,2b+1)} - \lambda_2^{(1,2b+1)} + f_b + g_b - u_b + r_b\\
0 &\leqslant \lambda_1^{(1,2b)} + u_b - g_b - s_b, g_b - u_b - s_b + r_b, \lambda_2^{(1,2b)} - u_b - r_b + s_b,\\
&\qquad k - \lambda_1^{(1,2b)} - \lambda_2^{(1,2b+1)} + s_b + r_b - u_b + f_b\\
0 &\leqslant u_b - r_b, \lambda_1^{(2b+1)} - u_b + r_b, f_b - u_b, k - \lambda_1^{(1,2b+1)} - \lambda_2^{(2b+1)} - u_b + g_b + s_b \qquad (25)\\
&\ \ \vdots\\
0 &\leqslant \lambda_1^{(\mathcal{N})} + v_{\mathcal{B}+1} - s_{\mathcal{B}+2}, s_{\mathcal{B}+2} - v_{\mathcal{B}+1}, \lambda_2^{(\mathcal{N})} - v_{\mathcal{B}+1} + g_{\mathcal{B}+1},\\
&\qquad k - \lambda_1^{(\mathcal{N})} - \lambda_2^{(1,\mathcal{N})} - v_{\mathcal{B}+1} + f_{\mathcal{B}+1} + r_{\mathcal{B}+2}\\
0 &\leqslant v_{\mathcal{B}+1} - g_{\mathcal{B}+1}, \lambda_1^{(1,\mathcal{N}-1)} - v_{\mathcal{B}+1} - g_{\mathcal{B}+1} + f_{\mathcal{B}+1}, g_{\mathcal{B}+1} - v_{\mathcal{B}+1} - f_{\mathcal{B}+1} + r_{\mathcal{B}+2},\\
&\qquad k - \lambda_1^{(1,\mathcal{N})} - \lambda_2^{(1,\mathcal{N}-1)} - v_{\mathcal{B}+1} + f_{\mathcal{B}+1} + g_{\mathcal{B}+1} + s_{\mathcal{B}+2}\\
0 &\leqslant \lambda_2^{(1,\mathcal{N}-1)} + v_{\mathcal{B}+1} - f_{\mathcal{B}+1} - r_{\mathcal{B}+2}, \lambda_2^{(\mathcal{N})} - v_{\mathcal{B}+1} - r_{\mathcal{B}+2} + s_{\mathcal{B}+2} + f_{\mathcal{B}+1},\\
&\qquad \lambda_1^{(1,\mathcal{N}-1)} - v_{\mathcal{B}+1} + r_{\mathcal{B}+2} - s_{\mathcal{B}+2}, k - \lambda_1^{(1,\mathcal{N})} - \lambda_2^{(1,\mathcal{N})} - v_{\mathcal{B}+1} + g_{\mathcal{B}+1} + s_{\mathcal{B}+2} + r_{\mathcal{B}+2}\\
0 &\leqslant \lambda_2^{(\mathcal{N}-1)} + u_{\mathcal{B}+1} - f_{\mathcal{B}+1}, \lambda_2^{(1,\mathcal{N}-2)} - u_{\mathcal{B}+1} - f_{\mathcal{B}+1} + g_{\mathcal{B}+1}, \lambda_1^{(\mathcal{N}-1)} - u_{\mathcal{B}+1} - g_{\mathcal{B}+1}\\
&\qquad + f_{\mathcal{B}+1} + s_{\mathcal{B}+1}, k - \lambda_2^{(1,\mathcal{N}-1)} - \lambda_1^{(1,\mathcal{N}-1)} - u_{\mathcal{B}+1} + f_{\mathcal{B}+1} + g_{\mathcal{B}+1} + r_{\mathcal{B}+1}\\
0 &\leqslant \lambda_1^{(1,\mathcal{N}-2)} + u_{\mathcal{B}+1} - g_{\mathcal{B}+1} - s_{\mathcal{B}+1}, g_{\mathcal{B}+1} - u_{\mathcal{B}+1} - s_{\mathcal{B}+1} + r_{\mathcal{B}+1}, \lambda_2^{(1,\mathcal{N}-2)} - u_{\mathcal{B}+1} + s_{\mathcal{B}+1} - r_{\mathcal{B}+1},\\
&\qquad k - \lambda_1^{(1,\mathcal{N}-2)} - \lambda_2^{(1,\mathcal{N}-1)} + f_{\mathcal{B}+1} + s_{\mathcal{B}+1} + r_{\mathcal{B}+1} - u_{\mathcal{B}+1}\\
0 &\leqslant u_{\mathcal{B}+1} - r_{\mathcal{B}+1}, \lambda_1^{(\mathcal{N}-1)} - u_{\mathcal{B}+1} + r_{\mathcal{B}+1}, f_{\mathcal{B}+1} - u_{\mathcal{B}+1},\\
&\qquad k - \lambda_1^{(1,\mathcal{N}-1)} - \lambda_2^{(\mathcal{N}-1)} + g_{\mathcal{B}+1} + s_{\mathcal{B}+1} - u_{\mathcal{B}+1}.
\end{aligned}
$$

Here b is a label defined in the interval $1 \leqslant b \leqslant \mathcal{B}$. The volume may be measured explicitly expressing $N^{(k,1)}_{\lambda^{(1)},\ldots,\lambda^{(\mathcal{N})}}$ as a multiple sum, with the appropriate order of summation:

$$
\begin{aligned}
N^{(k,1)}_{\lambda^{(1)},\ldots,\lambda^{(\mathcal{N})}} = &\left(\sum_{v_0}\sum_{s_1}\sum_{r_1}\right)\sum_{b}\left(\sum_{u_b}\sum_{g_b}\sum_{f_b}\sum_{v_b}\sum_{s_b+1}\sum_{r_b+1}\right)\\
&\times\sum_{u_{\mathcal{B}+1}}\sum_{g_{\mathcal{B}+1}}\sum_{f_{\mathcal{B}+1}}\sum_{v_{\mathcal{B}+1}}\sum_{s_{\mathcal{B}+2}}\sum_{r_{\mathcal{B}+2}} N^{(k,1)}_{\lambda^{(1,\mathcal{N})}-s_{\mathcal{B}}\alpha_1-r_{\mathcal{B}}\alpha_2}. \qquad (26)
\end{aligned}
$$

According to (21), the summand $N^{(k,1)}_{\lambda^{(1,\mathcal{N})}-s_{\mathcal{B}}\alpha_1-r_{\mathcal{B}}\alpha_2}$ may be expressed as

$$\begin{aligned}N^{(k,1)}_{\lambda^{(1,\mathcal{N})}-s_{\mathcal{B}}\alpha_1-r_{\mathcal{B}}\alpha_2} = \tfrac{1}{2}\Big(&\min\left\{\lambda_1^{(1,\mathcal{N})}-2s_{\mathcal{B}+2}+r_{\mathcal{B}+2},\lambda_2^{(1,\mathcal{N})}+s_{\mathcal{B}+2}-2r_{\mathcal{B}+2}\right\}+1\Big)\\ &\times\Big(k+2-\max\left\{\lambda_1^{(1,\mathcal{N})}-2s_{\mathcal{B}+2}+r_{\mathcal{B}+2},\lambda_2^{(1,\mathcal{N})}+s_{\mathcal{B}+2}-2r_{\mathcal{B}+2}\right\}\Big)\\ &\times\Big(k+1-\lambda_1^{(1,\mathcal{N})}-\lambda_2^{(1,\mathcal{N})}+s_{\mathcal{B}+2}+r_{\mathcal{B}+2}\Big).\end{aligned}\tag{27}$$

The lower bounds on the summation variables are

$$\begin{aligned}&v_0\geqslant 0\\ &s_1\geqslant\max\left\{\lambda_1^{(1)}+\lambda_2^{(1)}+\lambda_1^{(2)}+v_0-k,v_0\right\}\\ &r_1\geqslant\max\Big\{v_0,v_0-\lambda_1^{(1)}+s_1,\lambda_1^{(2)}+\lambda_2^{(2)}+\lambda_2^{(1)}+v_0-k,\lambda_2^{(1)}+\lambda_1^{(1)}+\lambda_2^{(2)}\\ &\qquad+\lambda_1^{(2)}-s_1+v_0-k\Big\},\\ &b\geqslant 1\\ &u_b\geqslant r_b\\ &g_b\geqslant\max\left\{u_b+s_b-r_b,\lambda_1^{(1,2b+1)}+\lambda_2^{(2b+1)}+u_b-s_b-k\right\}\\ &f_b\geqslant\max\Big\{\lambda_1^{(1,2b)}+\lambda_2^{(1,2b+1)}-s_b-r_b+u_b-k,\lambda_1^{(1,2b+1)}+\lambda_2^{(1,2b+1)}-g_b+u_b-r_b-k,\\ &\qquad u_b,u_b-\lambda_1^{(2b+1)}+g_b-s_b\Big\}\\ &v_b\geqslant g_b\\ &s_{b+1}\geqslant\max\left\{v_b,\lambda_1^{(1,2b+2)}+\lambda_2^{(1,2b+1)}-g_b-f_b+v_b-k\right\}\\ &r_{b+1}\geqslant\max\Big\{\lambda_1^{(2b+2)}+\lambda_2^{(1,2b+2)}+v_b-f_b-k,\lambda_1^{(1,2b+2)}+\lambda_2^{(1,2b+2)}-s_{b+1}+v_b-g_b-k,\\ &\qquad v_b-\lambda_1^{(1,2b+1)}+s_{b+1},v_b+f_b-g_b\Big\}\\ &u_{\mathcal{B}+1}\geqslant r_{\mathcal{B}+1}\\ &g_{\mathcal{B}+1}\geqslant\max\left\{\lambda_1^{(1,\mathcal{N}-1)}+\lambda_2^{(\mathcal{N}-1)}+u_{\mathcal{B}+1}-s_{\mathcal{B}+1}-k,u_{\mathcal{B}+1}+s_{\mathcal{B}+1}-r_{\mathcal{B}+1}\right\}\\ &f_{\mathcal{B}+1}\geqslant\max\Big\{\lambda_1^{(1,\mathcal{N}-2)}+\lambda_2^{(1,\mathcal{N}-1)}-s_{\mathcal{B}+1}-r_{\mathcal{B}+1}+u_{\mathcal{B}+1}-k,\lambda_1^{(1,\mathcal{N}-1)}+\lambda_2^{(1,\mathcal{N}-1)}-g_{\mathcal{B}+1}\\ &\qquad+u_{\mathcal{B}+1}-r_{\mathcal{B}+1}-k,u_{\mathcal{B}+1},u_{\mathcal{B}+1}-\lambda_1^{(\mathcal{N}-1)}+g_{\mathcal{B}+1}-s_{\mathcal{B}+1}\Big\}\\ &v_{\mathcal{B}+1}\geqslant g_{\mathcal{B}+1}\\ &s_{\mathcal{B}+2}\geqslant\max\left\{\lambda_1^{(1,\mathcal{N})}+\lambda_2^{(1,\mathcal{N}-1)}+v_{\mathcal{B}+1}-f_{\mathcal{B}+1}-g_{\mathcal{B}+1}-k,v_{\mathcal{B}+1}\right\}\\ &r_{\mathcal{B}+2}\geqslant\max\Big\{\lambda_1^{(1,\mathcal{N})}+\lambda_2^{(1,\mathcal{N})}+v_{\mathcal{B}+1}-g_{\mathcal{B}+1}-s_{\mathcal{B}+2}-k,v_{\mathcal{B}+1}-\lambda_1^{(1,\mathcal{N}-1)}+s_{\mathcal{B}+2},\\ &\qquad\lambda_1^{(\mathcal{N})}+\lambda_2^{(1,\mathcal{N})}+v_{\mathcal{B}+1}-f_{\mathcal{B}+1}-k,v_{\mathcal{B}+1}-g_{\mathcal{B}+1}+f_{\mathcal{B}+1}\Big\}.\end{aligned}\tag{28}$$

The upper bounds of the summation variables are

$$\begin{aligned}&v_0\leqslant\min\left\{\lambda_1^{(1)},\lambda_2^{(2)}\right\}\\ &s_1\leqslant\lambda_1^{(2)}+v_0\\ &r_1\leqslant\min\left\{\lambda_2^{(1)}+v_0,\lambda_2^{(2)}-v_0+s_1\right\}\end{aligned}$$

$$
\begin{aligned}
&b \leqslant \mathcal{B}\\
&u_b \leqslant \min\left\{\lambda_1^{(2b+1)} + r_b, \lambda_2^{(1,2b)} - r_b + s_b\right\}\\
&g_b \leqslant \lambda_1^{(1,2b)} + u_b - s_b\\
&f_b \leqslant \min\left\{\lambda_2^{(1,2b)} - u_b + g_b, \lambda_2^{(2b+1)} + u_b\right\}\\
&v_b \leqslant \min\left\{\lambda_1^{(1,2b+1)} - g_b + f_b, \lambda_2^{(2b+2)} + g_b\right\}\\
&s_{b+1} \leqslant \lambda_1^{(2b+2)} + v_b\\
&r_{b+1} \leqslant \min\left\{\lambda_2^{(1,2b+1)} + v_b - f_b, \lambda_2^{(2b+2)} - v_b + f_b + s_{b+1}\right\}\\
&u_{\mathcal{B}+1} \leqslant \min\left\{\lambda_2^{(1,\mathcal{N}-2)} + s_{\mathcal{B}+1} - r_{\mathcal{B}+1}, \lambda_1^{(\mathcal{N}-1)} + r_{\mathcal{B}+1}\right\}\\
&g_{\mathcal{B}+1} \leqslant \lambda_1^{(1,\mathcal{N}-2)} + u_{\mathcal{B}+1} - s_{\mathcal{B}+1}\\
&f_{\mathcal{B}+1} \leqslant \min\left\{\lambda_2^{(1,\mathcal{N}-2)} - u_{\mathcal{B}+1} + g_{\mathcal{B}+1}, \lambda_2^{(\mathcal{N}-1)} + u_{\mathcal{B}+1}\right\}\\
&v_{\mathcal{B}+1} \leqslant \min\left\{\lambda_2^{(\mathcal{N})} + g_{\mathcal{B}+1}, \lambda_1^{(1,\mathcal{N}-1)} - g_{\mathcal{B}+1} + f_{\mathcal{B}+1}\right\}\\
&s_{\mathcal{B}+2} \leqslant \lambda_1^{(\mathcal{N})} + v_{\mathcal{B}+1}\\
&r_{\mathcal{B}+2} \leqslant \min\left\{\lambda_2^{(1,\mathcal{N}-1)} + v_{\mathcal{B}+1} - f_{\mathcal{B}+1}, \lambda_2^{(\mathcal{N})} - v_{\mathcal{B}+1} + s_{\mathcal{B}+2} + f_{\mathcal{B}+1}\right\}.
\end{aligned}
\tag{29}
$$

The fusion multiplicity for $\mathcal{N}$ odd may be computed similarly. The associated diagram is similar to the even case (22) except that the second triangle from the right is turned upside down:

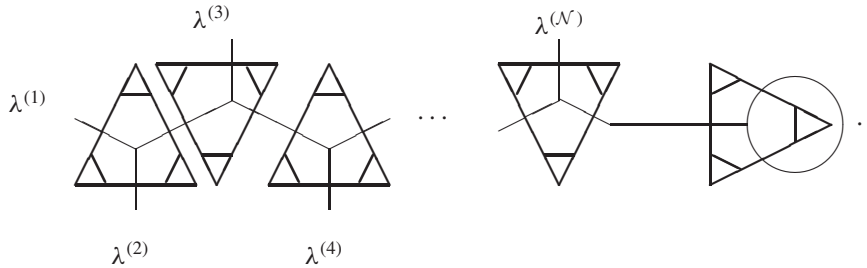

(30)

In this case, we let $\mathcal{B}$ count the number of pairs of triangles not involving $\lambda^{(1)}$, $\lambda^{(2)}$ or $\lambda^{(\mathcal{N})}$: $\mathcal{N} = 3 + 2\mathcal{B}$, i.e. $\mathcal{B} = \frac{1}{2}(\mathcal{N} - 3)$. Listing the inequalities, we have the following convex polytope:

$$
\begin{aligned}
&0 \leqslant \lambda_1^{(2)} + v_0 - s_1, s_1 - v_0, \lambda_2^{(2)} - v_0, k - \lambda_1^{(2)} - \lambda_2^{(2)} - \lambda_2^{(1)} + r_1 - v_0,\\
&0 \leqslant v_0, \lambda_1^{(1)} - v_0, r_1 - v_0, k - \lambda_1^{(1)} - \lambda_2^{(1)} - \lambda_1^{(2)} + s_1 - v_0,\\
&0 \leqslant \lambda_2^{(1)} + v_0 - r_1, \lambda_2^{(2)} - v_0 - r_1 + s_1, \lambda_1^{(1)} - v_0 + r_1 - s_1,\\
&\qquad\qquad k - \lambda_2^{(1)} - \lambda_2^{(2)} - \lambda_1^{(2)} - \lambda_1^{(1)} + r_1 + s_1 - v_0\\
&\quad\vdots\\
&0 \leqslant \lambda_1^{(2b+2)} + v_b - s_{b+1}, s_{b+1} - v_b, \lambda_2^{(2b+2)} - v_b + g_b, k - \lambda_2^{(1,2b+2)} - \lambda_1^{(1,2b+2)}\\
&\qquad\qquad + r_{b+1} + s_{b+1} - v_b + g_b\\
&0 \leqslant v_b - g_b, \lambda_1^{(1,2b+1)} - v_b - g_b + f_b, g_b - v_b - f_b + r_{b+1},\\
&\qquad\qquad k - \lambda_1^{(2b+2)} - \lambda_2^{(1,2b+2)} - v_b + f_b + r_{b+1}
\end{aligned}
$$

$$
\begin{aligned}
0 \leqslant\ & \lambda_2^{(1,2b+1)} + v_b - f_b - r_{b+1}, \lambda_2^{(2b+2)} - v_b + f_b - r_{b+1} + s_{b+1}, \lambda_1^{(1,2b+1)} - v_b + r_{b+1} - s_{b+1}, \\
& k - \lambda_1^{(1,2b+2)} - \lambda_2^{(1,2b+1)} + g_b + f_b - v_b + s_{b+1} \qquad (31)\\
0 \leqslant\ & \lambda_2^{(2b+1)} + u_b - f_b, \lambda_2^{(1,2b)} - u_b - f_b + g_b, \lambda_1^{(2b+1)} - u_b + f_b - g_b + s_b, \\
& k - \lambda_1^{(1,2b+1)} - \lambda_2^{(1,2b+1)} + f_b + g_b - u_b + r_b \\
0 \leqslant\ & \lambda_1^{(1,2b)} + u_b - g_b - s_b, g_b - u_b - s_b + r_b, \lambda_2^{(1,2b)} - u_b - r_b + s_b, \\
& k - \lambda_1^{(1,2b)} - \lambda_2^{(1,2b+1)} + s_b + r_b - u_b + f_b \\
0 \leqslant\ & u_b - r_b, \lambda_1^{(2b+1)} - u_b + r_b, f_b - u_b, k - \lambda_1^{(1,2b+1)} - \lambda_2^{(2b+1)} - u_b + g_b + s_b \\
& \vdots \\
0 \leqslant\ & \lambda_2^{(\mathcal{N})} + u_{\mathcal{B}+1} - f_{\mathcal{B}+1}, \lambda_2^{(1,\mathcal{N}-1)} - u_{\mathcal{B}+1} - f_{\mathcal{B}+1} + g_{\mathcal{B}+1}, \lambda_1^{(\mathcal{N})} - u_{\mathcal{B}+1} + f_{\mathcal{B}+1} - g_{\mathcal{B}+1} + s_{\mathcal{B}+1}, \\
& k - \lambda_2^{(1,\mathcal{N})} - \lambda_1^{(1,\mathcal{N})} + g_{\mathcal{B}+1} + f_{\mathcal{B}+1} - u_{\mathcal{B}+1} + r_{\mathcal{B}+1} \\
0 \leqslant\ & \lambda_1^{(1,\mathcal{N}-1)} + u_{\mathcal{B}+1} - g_{\mathcal{B}+1} - s_{\mathcal{B}+1}, g_{\mathcal{B}+1} - u_{\mathcal{B}+1} - s_{\mathcal{B}+1} + r_{\mathcal{B}+1}, \lambda_2^{(1,\mathcal{N}-1)} - u_{\mathcal{B}+1} \\
& + s_{\mathcal{B}+1} - r_{\mathcal{B}+1}, k - \lambda_1^{(\mathcal{N}-1)} - \lambda_2^{(1,\mathcal{N})} + s_{\mathcal{B}+1} + r_{\mathcal{B}+1} - u_{\mathcal{B}+1} + f_{\mathcal{B}+1} \\
0 \leqslant\ & u_{\mathcal{B}+1} - r_{\mathcal{B}+1}, \lambda_1^{(\mathcal{N})} - u_{\mathcal{B}+1} + r_{\mathcal{B}+1}, f_{\mathcal{B}+1} - u_{\mathcal{B}+1}, k - \lambda_1^{(1,\mathcal{N})} - \lambda_2^{(\mathcal{N})} - u_{\mathcal{B}+1} + g_{\mathcal{B}+1} + s_{\mathcal{B}+1}.
\end{aligned}
$$

As for $\mathcal{N}$ even, the volume may be measured explicitly expressing $N^{(k,1)}_{\lambda^{(1)},\ldots,\lambda^{(\mathcal{N})}}$ as a multiple sum, with the appropriate order of summation:

$$
N^{(k,1)}_{\lambda^{(1)},\ldots,\lambda^{(\mathcal{N})}} = \left(\sum_{v_0}\sum_{s_1}\sum_{r_1}\right)\sum_{b}\left(\sum_{u_b}\sum_{g_b}\sum_{f_b}\sum_{v_b}\sum_{s_b+1}\sum_{r_b+1}\right)\sum_{u_{\mathcal{B}+1}}\sum_{g_{\mathcal{B}+1}}\sum_{f_{\mathcal{B}+1}} N^{(k,1)}_{\lambda^{(1,\mathcal{N})}-g_{\mathcal{B}+1}\alpha_1-f_{\mathcal{B}+1}\alpha_2} \qquad (32)
$$

where the genus-1 1-point fusion multiplicity $N^{(k,1)}_{\lambda^{(1,\mathcal{N})}-g_{\mathcal{B}+1}\alpha_1-f_{\mathcal{B}+1}\alpha_2}$ is

$$
\begin{aligned}
N^{(k,1)}_{\lambda^{(1,\mathcal{N})}-g_{\mathcal{B}+1}\alpha_1-f_{\mathcal{B}+1}\alpha_2} =\ & \tfrac{1}{2}\left(\min\left\{\lambda_1^{(1,\mathcal{N})} - 2g_{\mathcal{B}+1} + f_{\mathcal{B}+1}, \lambda_2^{(1,\mathcal{N})} + g_{\mathcal{B}+1} - 2f_{\mathcal{B}+1}\right\} + 1\right) \\
& \times \left(k + 2 - \max\left\{\lambda_1^{(1,\mathcal{N})} - 2g_{\mathcal{B}+1} + f_{\mathcal{B}+1}, \lambda_2^{(1,\mathcal{N})} + g_{\mathcal{B}+1} - 2f_{\mathcal{B}+1}\right\}\right) \\
& \times \left(k + 1 - \lambda_1^{(1,\mathcal{N})} - \lambda_2^{(1,\mathcal{N})} + g_{\mathcal{B}+1} + f_{\mathcal{B}+1}\right). \qquad (33)
\end{aligned}
$$

The lower bounds of the summations are

$$
\begin{aligned}
& v_0 \geqslant 0 \\
& s_1 \geqslant \max\left\{\lambda_1^{(1)} + \lambda_2^{(1)} + \lambda_1^{(2)} + v_0 - k, v_0\right\} \\
& r_1 \geqslant \max\left\{v_0, v_0 - \lambda_1^{(1)} + s_1, \lambda_1^{(2)} + \lambda_2^{(2)} + \lambda_2^{(1)} + v_0 - k,\right. \\
& \qquad \left.\lambda_2^{(1)} + \lambda_1^{(1)} + \lambda_2^{(2)} + \lambda_1^{(2)} - s_1 + v_0 - k\right\} \\
& b \geqslant 1 \\
& u_b \geqslant r_b \\
& g_b \geqslant \max\left\{u_b + s_b - r_b, \lambda_1^{(1,2b+1)} + \lambda_2^{(2b+1)} + u_b - s_b - k\right\} \\
& f_b \geqslant \max\left\{\lambda_1^{(1,2b)} + \lambda_2^{(1,2b+1)} - s_b - r_b + u_b - k, \lambda_1^{(1,2b+1)} + \lambda_2^{(1,2b+1)} - g_b + u_b - r_b - k,\right. \\
& \qquad \left. u_b, u_b - \lambda_1^{(2b+1)} + g_b - s_b\right\} \qquad (34) \\
& v_b \geqslant g_b
\end{aligned}
$$

$$
\begin{aligned}
s_{b+1} &\geqslant \max\left\{v_b, \lambda_1^{(1,2b+2)} + \lambda_2^{(1,2b+1)} - g_b - f_b + v_b - k\right\}\\
r_{b+1} &\geqslant \max\left\{\lambda_1^{(2b+2)} + \lambda_2^{(1,2b+2)} + v_b - f_b - k, \lambda_1^{(1,2b+2)} + \lambda_2^{(1,2b+2)} - s_{b+1} + v_b - g_b - k,\right.\\
&\qquad \left. v_b - \lambda_1^{(1,2b+1)} + s_{b+1}, v_b + f_b - g_b\right\}\\
u_{\mathcal{B}+1} &\geqslant r_{\mathcal{B}+1}\\
g_{\mathcal{B}+1} &\geqslant \max\left\{\lambda_1^{(1,\mathcal{N})} + \lambda_2^{(\mathcal{N})} + u_{\mathcal{B}+1} - s_{\mathcal{B}+1} - k, u_{\mathcal{B}+1} + s_{\mathcal{B}+1} - r_{\mathcal{B}+1}\right\}\\
f_{\mathcal{B}+1} &\geqslant \max\left\{\lambda_1^{(1,\mathcal{N}-1)} + \lambda_2^{(1,\mathcal{N})} - s_{\mathcal{B}+1} - r_{\mathcal{B}+1} + u_{\mathcal{B}+1} - k, \lambda_1^{(1,\mathcal{N})} + \lambda_2^{(1,\mathcal{N})} - g_{\mathcal{B}+1}\right.\\
&\qquad \left. + u_{\mathcal{B}+1} - r_{\mathcal{B}+1} - k, u_{\mathcal{B}+1}, u_{\mathcal{B}+1} - \lambda_1^{(\mathcal{N})} + g_{\mathcal{B}+1} - s_{\mathcal{B}+1}\right\}.
\end{aligned}
$$

The upper bounds of the summations are

$$
\begin{aligned}
v_0 &\leqslant \min\left\{\lambda_1^{(1)}, \lambda_2^{(2)}\right\}\\
s_1 &\leqslant \lambda_1^{(2)} + v_0\\
r_1 &\leqslant \min\left\{\lambda_2^{(1)} + v_0, \lambda_2^{(2)} - v_0 + s_1\right\}\\
b &\leqslant \mathcal{B}\\
u_b &\leqslant \min\left\{\lambda_1^{(2b+1)} + r_b, \lambda_2^{(1,2b)} - r_b + s_b\right\}\\
g_b &\leqslant \lambda_1^{(1,2b)} + u_b - s_b\\
f_b &\leqslant \min\left\{\lambda_2^{(1,2b)} - u_b + g_b, \lambda_2^{(2b+1)} + u_b\right\}\\
v_b &\leqslant \min\left\{\lambda_1^{(1,2b+1)} - g_b + f_b, \lambda_2^{(2b+2)} + g_b\right\}\\
s_{b+1} &\leqslant \lambda_1^{(2b+2)} + v_b\\
r_{b+1} &\leqslant \min\left\{\lambda_2^{(1,2b+1)} + v_b - f_b, \lambda_2^{(2b+2)} - v_b + f_b + s_{b+1}\right\}\\
u_{\mathcal{B}+1} &\leqslant \min\left\{\lambda_2^{(1,\mathcal{N}-1)} + s_{\mathcal{B}+1} - r_{\mathcal{B}+1}, \lambda_1^{(\mathcal{N})} + r_{\mathcal{B}+1}\right\}\\
g_{\mathcal{B}+1} &\leqslant \lambda_1^{(1,\mathcal{N}-1)} + u_{\mathcal{B}+1} - s_{\mathcal{B}+1}\\
f_{\mathcal{B}+1} &\leqslant \min\left\{\lambda_2^{(1,\mathcal{N}-1)} - u_{\mathcal{B}+1} + g_{\mathcal{B}+1}, \lambda_2^{(\mathcal{N})} + u_{\mathcal{B}+1}\right\}.
\end{aligned}
\tag{35}
$$

These results constitute the first explicit results for higher-genus $\mathcal{N}$-point $su(3)$ fusion multiplicities. For general $h > 1$, the polytope characterization of $su(3)$ fusion multiplicities is straightforward, but very cumbersome and will not be discussed explicitly here. In the next section we will consider briefly the extension to $su(N)$, while the appendix contains details on $su(4)$.

We conclude this section by writing down a double-sum formula for the genus-2 0-point $su(3)$ fusion multiplicity. It is obtained by gluing two genus-1 1-point fusions (21) together, and summing over the internal weight subject to the conditions following (21). We find

$$
N^{(k,2)} = \sum_{i=0}^{[k/2]} \sum_{j=0}^{[(k-2i)/3]} \left(\frac{1}{2}(i+1)(k+2-i-3j)(k+1-2i-3j)\right)^2 \tag{36}
$$

where $[x]$ denotes the integer value of x, i.e. the greatest integer less than or equal to x. This double sum may be summed explicitly, and we find that the genus-2 0-point $su(3)$ fusion multiplicity is a simple binomial coefficient in the affine level k:

$$N^{(k,2)} = \binom{k+8}{k} \tag{37}$$

This is believed to be the first concise result on fusion multiplicities for $r, h > 1$.

4. On higher-genus $su(N)$ fusion

Pending the explicit assignment of threshold levels to true BZ triangles for $N > 4$, our method allows us to characterize all higher-genus $\mathcal{N}$-point $su(N)$ fusion multiplicities by convex polytopes. Let us indicate how by considering the genus-h $\mathcal{N}$-point diagram

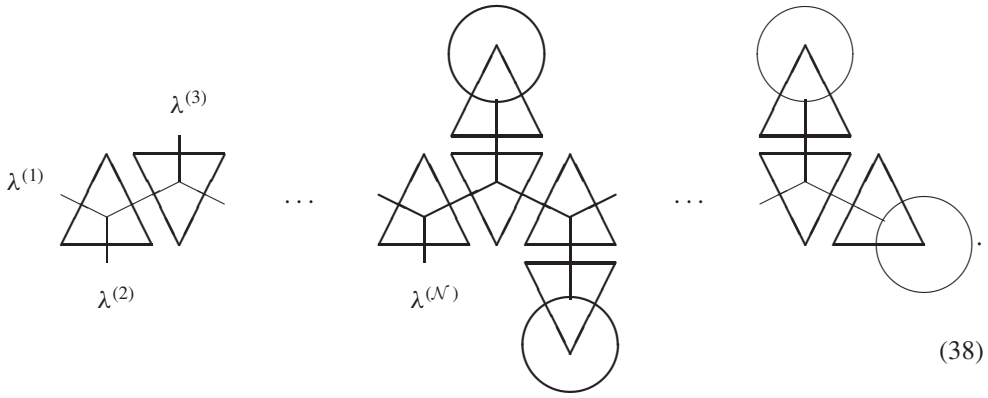

(38)

In this particular example, $\mathcal{N}$ and h are assumed even.

For $h, \mathcal{N} > 0$, the number of glued triangles is $\mathcal{N} + 2h - 2$. Thus, assuming that the assignment of threshold levels, t_q, to the individual triangles, $\mathcal{T}_q$, is known, we have the level-dependent inequalities

$$t_q \leqslant k \qquad q = 1, \ldots, \mathcal{N} + 2h - 2. \tag{39}$$

All other conditions follow from demanding that all entries must be *non-negative* integers. This leads to

$$(\mathcal{N} + 2h - 2)E_r = \tfrac{3}{2}(\mathcal{N} + 2h - 2)r(r+1) \tag{40}$$

level-independent inequalities. The entries and threshold levels are given in terms of an initial diagram $\mathcal{D}_0$, the $(\mathcal{N} + 2h - 2)H_r$ virtual triangle parameters v, the $(\mathcal{N} + 2h - 3)r$ gluing parameters g and the hr loop-gluing parameters l. In a self-explanatory notation, we have

$$\mathcal{D} = \mathcal{D}_0 + \sum_{a=1}^{\mathcal{N}+2h-2} \sum_{i,j=1}^{i+j=r} v_{i,j}^{(a)} \mathcal{V}_{i,j}^{(a)} + \sum_{a=1}^{\mathcal{N}+2h-3} \sum_{i=1}^{r} g_i^{(a)} \mathcal{G}_i^{(a)} + \sum_{a=1}^{h} \sum_{i=1}^{r} l_i^{(a)} \mathcal{L}_i^{(a)}. \tag{41}$$

The sign convention is immaterial. We see that the polytope is embedded in the Euclidean space $\mathbb{R}^{r((h-1)(r+2)+\mathcal{N}(r+1)/2)}$.

The initial diagram $\mathcal{D}_0$ depends only on the $\mathcal{N}$ outer weights $\lambda^{(1)}, \ldots, \lambda^{(\mathcal{N})}$. A convenient choice is characterized by having vanishing entries to the right of the $(\mathcal{N} - 1)$th triangle in (38) (counting from the left). The entries of the remaining $\mathcal{N} - 1$ (leftmost) triangles follow

the description of genus-0 $(\mathcal{N}+1)$-point diagrams in [2], with a vanishing $(\mathcal{N}+1)$th weight being located on the triangle edge along which we just imagined the diagram (38) to be cut.

This concludes the characterization of genus-h $\mathcal{N}$-point $su(N)$ fusion multiplicities by polytopes. The discretized volume of the polytope associated with a generic higher-genus fusion multiplicity is in general not straightforward to measure, and will not be addressed further here. By construction, however, it gives the fusion multiplicity $N^{(k,h)}_{\lambda^{(1)},\ldots,\lambda^{(\mathcal{N})}}$.

Of particular interest are the genus-1 0-point fusion multiplicities $N^{(k,1)}$, which depend solely on the affine level k and the rank r of $su(r+1)$. They also provide a nice check of our general picture. Our approach simplifies radically in that case. We are considering the tadpole diagram (8) with vanishing outer weight for which there is no gluing, only a single loop gluing. Thus, the parameters g in (41) vanish. Furthermore, the initial diagram $\mathcal{D}_0$ may be chosen to have vanishing entries only. From the structure of the basis virtual triangles and loop-gluing diagrams, it then follows that all the v parameters vanish as well. The associated polytope is then characterized by the inequalities

$$0 \leqslant l_1, \ldots, l_r \qquad t(l_1, \ldots, l_r) \leqslant k. \tag{42}$$

The threshold level $t(l_1, \ldots, l_r)$ is now a function of the loop-gluing parameters only. In all known cases, it is a first-order expression in the entries, cf. (15) and (49). It need not be linear, though. Assuming that this first-order dependence generalizes to all $su(N)$, we see that the genus-1 0-point fusion multiplicity is polynomial in the level k, of degree less than or equal to the rank $r = N-1$. Let us list the lower-rank cases (see [3] for $su(2)$, (21) for $su(3)$ and (57) for $su(4)$):

$$\begin{aligned} r=1: &\quad N^{(k,1)} = k+1 \\ r=2: &\quad N^{(k,1)} = \tfrac{1}{2}(k+1)(k+2) \\ r=3: &\quad N^{(k,1)} = \tfrac{1}{6}(k+1)(k+2)(k+3). \end{aligned} \tag{43}$$

It is natural to expect that for general rank, the fusion multiplicity is

$$N^{(k,1)} = \binom{k+r}{r}. \tag{44}$$

Indeed, this is the result by the Verlinde formula:

$$N^{(k,h)}_{\lambda^{(1)},\ldots,\lambda^{(\mathcal{N})}} = \sum_{\sigma \in P^k_+} (S_{0,\sigma})^{2(1-h)} \left(\frac{S_{\lambda^{(1)},\sigma}}{S_{0,\sigma}}\right) \cdots \left(\frac{S_{\lambda^{(\mathcal{N})},\sigma}}{S_{0,\sigma}}\right) \tag{45}$$

where P^k_+ is the set of integrable affine highest weights at level k. With $\mathcal{N}=0$ and $h=1$, $N^{(k,1)}$ counts the number of primary fields in a Wess–Zumino–Witten conformal field theory at level k, which is exactly (44).

5. Conclusion

We have provided a prescription for characterizing higher-genus $\mathcal{N}$-point $su(N)$ fusion multiplicities as discretized polytope volumes. Our method is based on techniques of gluing BZ triangles together to form multi-sided diagrams. In order to treat higher-genus fusion, we introduced a complete basis of loop-gluing diagrams for all $su(N)$. The remaining input is a knowledge of threshold levels of the various couplings. The assignment of threshold levels to BZ triangles is known for $N = 2, 3, 4$. We therefore put particular emphasis on $su(3)$ and $su(4)$, but also discussed the general case, assuming that the issue of threshold levels was settled.

An alternative approach to fusion discussed in [12] and based on [13–16], amounts to analysing three-point functions in Wess–Zumino–Witten conformal field theory. Due to its universal nature, this method allows one to treat other Lie algebras than $su(N)$ as well. So far, only lower-rank cases have been considered explicitly.

Related approaches to characterize fusion multiplicities by polytopes were considered in [17, 18]. However, the complexity of all known methods increases rapidly with the rank of the Lie algebra. It is therefore natural to expect that further progress will depend on novel insight, or an ingenious hybrid of the existing techniques.

Finally, let us point out that all of our multiple-sum formulas for fusion multiplicities can be rewritten as formulas for the so-called exponential sums of the corresponding polytopes. These exponential sums are very important in polytope theory [19], and lead to the possibility that our discrete polytope volume picture admits a sensible description in terms of residue formulas (other fusion residue formulas have been written in [20]). We hope to report on this in the future.

Acknowledgments

JR thanks Frédéric Lesage for helpful discussions. The work of MAW is supported by NSERC, and that of JR by a CRM-ISM postdoctoral fellowship. GF and MT were supported in part by NSERC undergraduate student research awards.

Appendix. Higher-genus $su(4)$ fusion

An $su(4)$ BZ triangle is defined in terms of 18 non-negative integers:

$$\begin{array}{ccccccccccc}
 & & & & & m_{14} & & & & & \\
 & & & & n_{12} & & l_{34} & & & & \\
 & & & m_{24} & & & & m_{13} & & & \\
 & & n_{13} & & l_{23} & & n_{23} & & l_{24} & & \\
 & m_{34} & & & & m_{23} & & & & m_{12} & \\
n_{14} & & l_{12} & & n_{24} & & l_{13} & & n_{34} & & l_{14}
\end{array} \tag{46}$$

related to the Dynkin labels by

$$\begin{array}{lll}
m_{14}+n_{12}=\lambda_1 & n_{14}+l_{12}=\mu_1 & l_{14}+m_{12}=\nu_1 \\
m_{24}+n_{13}=\lambda_2 & n_{24}+l_{13}=\mu_2 & l_{24}+m_{13}=\nu_2 \\
m_{34}+n_{14}=\lambda_3 & n_{34}+l_{14}=\mu_3 & l_{34}+m_{14}=\nu_3.
\end{array} \tag{47}$$

The $su(4)$ BZ triangle contains three hexagons with the associated constraints

$$\begin{array}{lll}
n_{12}+m_{24}=m_{13}+n_{23} & n_{13}+l_{23}=l_{12}+n_{24} & l_{24}+n_{23}=l_{13}+n_{34} \\
n_{12}+l_{34}=l_{23}+n_{23} & n_{13}+m_{34}=n_{24}+m_{23} & n_{23}+m_{23}=m_{12}+n_{34} \\
m_{24}+l_{23}=l_{34}+m_{13} & m_{34}+l_{12}=l_{23}+m_{23} & l_{13}+m_{23}=l_{24}+m_{12}.
\end{array} \tag{48}$$

Only six of these nine hexagon identities are independent. We can assign the threshold level to (46) as follows:

$$\begin{aligned}
t=\max\big\{&\lambda_1+\lambda_2+\lambda_3+l_{14},\,\mu_1+\mu_2+\mu_3+m_{14},\,\nu_1+\nu_2+\nu_3+n_{14},\\
&\lambda_1+\lambda_2+l_{14}+l_{24}+n_{14},\,\lambda_2+\lambda_3+l_{14}+l_{13}+m_{14},\\
&\mu_1+\mu_2+m_{14}+m_{24}+l_{14},\,\mu_2+\mu_3+m_{14}+m_{13}+n_{14},\\
&\nu_1+\nu_2+n_{14}+n_{24}+m_{14},\,\nu_2+\nu_3+n_{14}+n_{13}+l_{14},\\
&l_{14}+m_{14}+n_{14}+\left[\tfrac{1}{2}(\lambda_2+\mu_2+\nu_2+l_{23}+m_{23}+n_{23}+1)\right]\big\}.
\end{aligned} \tag{49}$$

The discretized volume of the convex polytope (in v_1, v_2 and v_3) subject to the inequalities

$$\begin{aligned}0 \leqslant\ & v_2, \mu_1 - v_2, \lambda_3 - v_2, -v_2 + v_3, v_1 - v_2, \mu_2 + v_2 - v_3, \lambda_2 - v_1 + v_2, \lambda_3 + v_1 - v_2 - v_3,\\ & \mu_1 - v_1 - v_2 + v_3, n_1 - v_3, n_2 - v_1 + v_2 - v_3, n_3 - v_1, N_1 + v_3, N_1' - v_3,\\ & N_2 + v_1 - v_3, N_2' - v_1 + v_3, N_3 - v_1, N_3' + v_1, k - \lambda_1 - \lambda_2 - \lambda_3 - N_1 - v_3,\\ & k - \mu_1 - \mu_2 - \mu_3 - N_3' - v_1, k - \nu_1 - \nu_2 - \nu_3 - v_2,\\ & k - \lambda_1 - \lambda_2 - N_1 - N_2 - v_1 - v_2, k - \mu_2 - \mu_3 - N_2' - N_3' - v_2 - v_3,\\ & k + \lambda_3 - \nu_1 - \nu_2 - \nu_3 - v_2 - v_3, k + \mu_1 - \nu_1 - \nu_2 - \nu_3 - v_1 - v_2,\\ & k - \nu_1 - \nu_2 - N_3' - v_1 - v_3, k - \nu_2 - \nu_3 - N_1 - v_1 - v_3,\\ & 2k - \lambda^1 + \lambda^3 + \mu^1 - \mu^3 - \nu^1 - \nu^2 - \nu^3 - v_1 - v_2 - v_3 \end{aligned} \tag{50}$$

is the fusion multiplicity $N^{(k)}_{\lambda,\mu,\nu}$. We refer to [4] for an explicit multiple-sum formula measuring this volume. Here, the parameters are defined as follows:

$$\begin{aligned} n_1 &= \lambda^3 + \mu^3 - \nu^1\\ n_2 &= \lambda^2 + \mu^2 - \nu^2\\ n_3 &= \lambda^1 + \mu^1 - \nu^3\\ N_1 &= -n_1 + \mu_3\\ N_2 &= n_1 - n_2 + \mu_2\\ N_3 &= n_2 - n_3 + \mu_1\\ N_1' &= \nu_1 - N_1\\ N_2' &= \nu_2 - N_2\\ N_3' &= \nu_3 - N_3 \end{aligned} \tag{51}$$

where the dual Dynkin labels can be written as $\lambda^1 = \frac{1}{4}(3\lambda_1+2\lambda_2+\lambda_3)$, $\lambda^2 = \frac{1}{4}(2\lambda_2+4\lambda_2+2\lambda_3)$ and $\lambda^3 = \frac{1}{4}(\lambda_1 + 2\lambda_2 + 3\lambda_3)$. μ^i and ν^i are defined similarly.

Now we focus on the genus-1 1-point $su(4)$ fusion. The method for finding the discretized volume of the associated convex polytope is the same as for $su(3)$. In this case we have three virtual triangles and three loop-gluing diagrams as shown in (11). For the genus-1 1-point fusion this defines the diagram

$$\mathcal{D} = \mathcal{D}_0 + \sum_{i=1}^{3} v_i \mathcal{V}_i - \sum_{j=1}^{3} l_i \mathcal{L}_i \tag{52}$$

with associated convex polytope

$$\begin{aligned}0 \leqslant\ & \lambda_1 + v_2, -v_2 \qquad -\tfrac{1}{4}(\lambda_1 - 2\lambda_2 - \lambda_3) - v_2 + v_3, k - \lambda_1 - \lambda_2 - \lambda_3 + l_1 - v_1,\\ & k - \tfrac{1}{4}(7\lambda_1 + 2\lambda_2 + \lambda_3) + l_1 + l_2 + l_3 - v_2\\ 0 \leqslant\ & \tfrac{1}{4}(\lambda_1 + 2\lambda_2 - \lambda_3) + v_2 - v_3, -\tfrac{1}{2}(\lambda_1 - \lambda_3) - v_3, \tfrac{1}{2}(\lambda_1 + \lambda_3) + v_3, k - \tfrac{1}{4}(5\lambda_1 + 2\lambda_2 + 3\lambda_3)\\ & + l_1 + l_2 + l_3 - v_3, k - \lambda_1 - \lambda_2 - \lambda_3 + l_1 + l_2 - v_1 - v_3\\ 0 \leqslant\ & \tfrac{1}{2}(\lambda_1 - \lambda_3) - v_3 - l_3, -\tfrac{1}{4}(\lambda_1 - 2\lambda_2 - \lambda_3) - v_3 + v_1, v_3 - v_1 - l_2, -v_1,\\ & k - \tfrac{1}{4}(6\lambda_1 + 4\lambda_2 + 2\lambda_3) + l_1 + l_2 + l_3 - v_1 - v_2,\\ & k - \tfrac{1}{4}(6\lambda_1 + 4\lambda_2 + 2\lambda_3) + l_1 + l_2 - v_2 - v_3\\ 0 \leqslant\ & -l_1 + v_1, v_2 - v_1 - l_2, -\tfrac{1}{4}(\lambda_1 - 2\lambda_2 - \lambda_3) + v_1 - v_2,\\ & k - \lambda_1 - \lambda_2 - \lambda_3 + l_1 + l_2 - v_2 - v_3,\\ & k - \tfrac{1}{4}(6\lambda_1 + 4\lambda_2 + 2\lambda_3) + l_1 + l_2 + l_3 - v_1 - v_3 \end{aligned} \tag{53}$$

$$\begin{aligned}0 \leqslant\ & -v_2 - l_3,\, v_1 - v_2 - v_3 - l_3,\, v_2 - v_1 - v_3,\, v_3 - v_1 - v_2,\\ & k - \lambda_1 - \lambda_2 - \lambda_3 + l_1 + l_2 - v_1 - v_3,\\ & 2k - \tfrac{1}{4}(10\lambda_1 + 8\lambda_2 + 6\lambda_3) - v_1 - v_2 - v_3 + 2l_1 + 2l_2 + l_3.\end{aligned}$$

The fusion multiplicity $N_\lambda^{(k,1)}$ can now be expressed as a multiple sum as follows:

$$N_\lambda^{(k,1)} = \sum_{v_3}\sum_{v_2}\sum_{v_1}\sum_{l_1}\sum_{l_2}\sum_{l_3} 1. \tag{54}$$

The lower bounds of the summation variables are

$$\begin{aligned}
&v_3 \geqslant -\tfrac{1}{2}(\lambda_1 + \lambda_3)\\
&v_2 \geqslant \max\left\{-\lambda_1, -\tfrac{1}{4}(\lambda_1 + 2\lambda_2 - \lambda_3) + v_3\right\}\\
&v_1 \geqslant \max\left\{\tfrac{1}{4}(\lambda_1 - 2\lambda_2 - \lambda_3) + v_2, \tfrac{1}{4}(\lambda_1 - 2\lambda_2 - \lambda_3) + v_3\right\}\\
&l_1 \geqslant \lambda_1 + \lambda_2 + \lambda_3 + v_1 - k\\
&l_2 \geqslant \max\big\{\lambda_1 + \lambda_2 + \lambda_3 - l_1 + v_1 + v_2 - k,\, \tfrac{1}{4}(6\lambda_1 + 4\lambda_2 + 2\lambda_3) - l_1 + v_2 + v_3 - k,\\
&\qquad \lambda_1 + \lambda_2 + \lambda_3 - l_1 + v_2 + v_3 - k,\, \lambda_1 + \lambda_2 + \lambda_3 - l_1 + v_1 + v_3 - k\big\}\\
&l_3 \geqslant \max\left\{\tfrac{1}{4}(7\lambda_1 + 2\lambda_2 + \lambda_3) - l_1 - l_2 + v_2 - k,\, \tfrac{1}{4}(5\lambda_1 + 2\lambda_2 + 3\lambda_3) - l_2 + v_3 - l_1 - k,\right.\\
&\qquad \tfrac{1}{4}(6\lambda_1 + 4\lambda_2 + 2\lambda_3) - l_1 - l_2 + v_1 + v_2 - k,\\
&\qquad \tfrac{1}{4}(6\lambda_1 + 4\lambda_2 + 2\lambda_3) - l_1 - l_2 + v_1 + v_2 - k,\\
&\qquad \left.\tfrac{1}{4}(10\lambda_1 + 8\lambda_2 + 6\lambda_3) + v_1 + v_2 + v_3 - 2l_1 - 2l_2 - 2k\right\}.
\end{aligned} \tag{55}$$

The upper bounds of the summation variables are

$$\begin{aligned}
&v_3 \leqslant -\tfrac{1}{2}(\lambda_1 - \lambda_3)\\
&v_2 \leqslant \min\left\{0, -\tfrac{1}{4}(\lambda_1 - 2\lambda_2 - \lambda_3) + v_3\right\}\\
&v_1 \leqslant \min\{0, v_2 - v_3, v_3 - v_2\}\\
&l_1 \leqslant v_1\\
&l_2 \leqslant \min\{v_3 - v_1, v_2 - v_1\}\\
&l_3 \leqslant \min\left\{v_1 - v_2 - v_3, -v_2, \tfrac{1}{2}(\lambda_1 - \lambda_3) - v_3\right\}.
\end{aligned} \tag{56}$$

Specializing to $\lambda = 0$, we work out the multi-summation and find the genus-1 0-point fusion multiplicity

$$N^{(k,1)} = \sum_{l_1=0}^{k}\sum_{l_2=0}^{k-l_1}\sum_{l_3=0}^{k-l_1-l_2} 1 = \frac{1}{6}(k+1)(k+2)(k+3). \tag{57}$$

To conclude this section, we will state how the genus-2 0-point fusion multiplicity may be characterized as the discretized volume of a polytope. In this case, the associated diagram can be written as

$$\mathcal{D} = \mathcal{D}_0 + \sum_{i=1}^{6} v_i \mathcal{V}_i - \sum_{j=1}^{3} g_j \mathcal{G}_j - \sum_{k=1}^{6} l_k \mathcal{L}_k. \tag{58}$$

The initial diagram $\mathcal{D}_0$ may be chosen to have only vanishing entries, and the associated convex polytope becomes

$$\begin{aligned}0 \leqslant\ & v_2 - g_1,\, g_2 - g_1 - v_2,\, v_3 - v_2 + g_1 - g_2,\, k - v_3 + g_3 + l_1 + l_2 + l_3,\, k - v_1 + l_1 + g_1 + g_3\\
0 \leqslant\ & v_2 - v_3 - g_2 + g_3,\, g_2 - g_3 - v_3,\, v_3 - g_3,\, k - v_2 + g_1 + l_1 + l_3,\\
& k - v_1 - v_2 + g_1 + g_3 + l_1 + l_2\end{aligned}$$

$$
\begin{aligned}
0 \leqslant\ & g_3 - v_3 - l_3,\ v_1 - v_3,\ v_3 - v_1 - l_2,\ k - v_2 - v_1 + g_2 + l_1 + l_2 + l_3,\\
& k - v_2 - v_3 + g_1 + g_2 + l_1 + l_2\\
0 \leqslant\ & v_1 - l_1,\ -v_1,\ v_2 - v_1 - l_2,\ v_1 - v_2,\ k - v_2 - v_3 + g_2 + g_3 + l_1 + l_2,\\
& k - v_1 - v_3 + g_2 + l_1 + l_2 + l_3\\
0 \leqslant\ & g_1 - v_2 - l_3,\ g_2 - v_2 - v_3 - l_3,\ -v_1 - v_2,\ -v_1 - v_3,\ k - v_1 - v_3 + l_1 + l_2 + g_1 + g_3,\\
& 2k + g_1 + g_2 + g_3 + 2l_1 + 2l_2 + l_3\\
0 \leqslant\ & v_4 - g_1,\ g_2 - g_1 - v_4,\ v_5 - v_4 + g_1 - g_2,\ k - v_6 + g_1 + g_3 + l_4,\\
& k - v_4 + g_1 + l_4 + l_5 + l_6\\
0 \leqslant\ & v_4 - v_5 - g_2 + g_3,\ g_2 - g_3 - v_5,\ v_5 - g_3,\ k - v_5 + g_3 + l_4 + l_5 + l_6,\\
& k - v_5 - v_6 + g_1 + g_3 + l_4 + l_5\\
0 \leqslant\ & g_3 - v_5 - l_6,\ v_6 - v_5,\ v_5 - v_6 - l_5,\ k - v_5 - v_6 + g_2 + l_4 + l_5 + l_6,\\
& k - v_4 - v_5 + l_4 + l_5 + g_2 + g_3\\
0 \leqslant\ & v_6 - l_4,\ -v_6,\ v_4 - v_6 - l_5,\ v_6 - v_4,\ k - v_4 - v_5 + l_4 + l_5 + g_1 + g_2,\\
& k - v_4 - v_6 + g_2 + l_4 + l_5 + l_6\\
0 \leqslant\ & g_1 - v_4 - l_6,\ g_2 - v_4 - v_5 - l_6,\ -v_6 - v_4,\ -v_6 - v_5,\ k - v_4 - v_6 + g_1 + g_3 + l_4 + l_5,\\
& 2k - v_4 + g_1 + g_3 + 2l_4 + 2l_5 + l_6.
\end{aligned}
\tag{59}
$$

This is an example where measuring the discretized volume of the polytope requires analysing intersections of the polytope faces (in the terminology of [1], there is no appropriate order of summation). That is in principle straightforward, but will not be carried out here.

References

[1] Rasmussen J and Walton M A 2001 *su*(*N*) tensor product multiplicities and virtual Berenstein–Zelevinsky triangles *J. Phys. A: Math. Gen.* **34** 11095 (*Preprint* math-ph/0010051)

[2] Rasmussen J and Walton M A 2001 Higher *su*(*N*) tensor products *J. Phys. A: Math. Gen.* **34** 7685 (*Preprint* math-ph/0102031)

[3] Rasmussen J and Walton M A 2002 Fusion multiplicities as polytope volumes: $\mathcal{N}$-point and higher-genus *su*(2) fusion *Nucl. Phys.* B **620** 537 (*Preprint* hep-th/0104240)

[4] Rasmussen J and Walton M A 2002 Affine *su*(3) and *su*(4) fusion multiplicities as polytope volumes *J. Phys. A: Math. Gen.* **35** 6939

[5] Berenstein A D and Zelevinsky A V 1992 Triple multiplicities for SL(r + 1) and the spectrum of the exterior algebra of the adjoint representation *J. Algebr. Comb.* **1** 7

[6] Cummins C J, Mathieu P and Walton M A 1991 Generating functions for WZNW fusion rules *Phys. Lett.* B **254** 386

[7] Kirillov A N, Mathieu P, Sénéchal D and Walton M A 1993 Group-theoretical methods in physics *Proc. 19th Int. Colloquium (Salamanca, Spain, 1992)* vol 1 (Madrid: CIEMAT)

[8] Bégin L, Kirillov A N, Mathieu P and Walton M A 1993 Berenstein–Zelevinsky triangles, elementary couplings and fusion rules *Lett. Math. Phys.* **28** 257 (*Preprint* hep-th/9301075)

[9] Rasmussen J 2002 $\mathcal{N}$-point and higher-genus *osp*(1|2) fusion *Preprint* hep-th/0205322

[10] Verlinde E 1988 Fusion rules and modular transformations in 2D conformal field theory *Nucl. Phys.* B **300** 360

[11] Irvine S E and Walton M A 2000 Schubert calculus and threshold polynomials of affine fusion *Nucl. Phys.* B **504** 795

[12] Rasmussen J and Walton M A 2001 On the level-dependence of Wess–Zumino–Witten three-point functions *Nucl. Phys.* B **616** 517 (*Preprint* hep-th/0105294)

[13] Rasmussen J 1996 Applications of free fields in 2D current algebra *PhD thesis* Niels Bohr Institute (*Preprint* hep-th/9610167)

[14] Petersen J L, Rasmussen J and Yu M 1997 Free field realizations of 2D current algebras, screening currents and primary fields *Nucl. Phys.* B **502** 649 (*Preprint* hep-th/9704052)

[15] Rasmussen J 1998 Two-point functions in affine SL(N) current algebra *Mod. Phys. Lett.* A **13** 1213 (*Preprint* hep-th/9803114)
Rasmussen J 1998 Two-point functions in affine current algebra and conjugate weights *Mod. Phys. Lett.* A **13** 1281 (*Preprint* hep-th/9803182)
[16] Rasmussen J 1999 Three-point functions in conformal field theory with affine Lie group symmetry *Int. J. Mod. Phys.* A **14** 1225 (*Preprint* hep-th/9807153)
[17] Bégin L, Cummins C, Lapointe L and Mathieu P 2001 Fusion bases as facets of polytopes *Preprint* hep-th/0108213
[18] Rasmussen J and Walton M A 2002 Purely affine elementary $su(N)$ fusions *Mod. Phys. Lett.* A **17** 1249 (*Preprint* hep-th/0110223)
[19] Barvinok A 1997 Lattice Points and Lattice Polytopes *Handbook of Discrete and Computational Geometry* ed J Goodman and J O'Rourke (Boca Raton, FL: CRC Press) pp 133–52
[20] Intriligator K 1991 Fusion residues *Mod. Phys. Lett.* A **6** 3543 (*Preprint* hep-th/9108005)
Szenes A 1994 *The Combinatorics of the Verlinde Formulas London Math. Soc. Lecture Note Ser. vol 208* (Cambridge: Cambridge University Press) p 241 (*Preprint* alg-geom/9402003)